NJC

ROYAL SOCIETY OF CHEMISTRY

PAPER

View Article Online
View Journal | View Issue

Cite this: *New J. Chem.*, 2020, **44**, 9703

A zwitterionic polymer containing a hydrophobic group: enhanced rheological properties†

Ling Liu,[a] Shaohua Gou,*[ab] Huichao Zhang,[c] Lihua Zhou,[a] Lan Tang[a] and Lang Liu[a]

Received 4th April 2020,
Accepted 17th May 2020

DOI: 10.1039/d0nj01687j

rsc.li/njc

A zwitterionic polymer containing a hydrophobic long chain, named MANPS, was independently developed by free radical solution polymerization. The introduction of an hydrophobic long-chain monomer, namely, octadec-9-enioc acid allylamide (NAE) and an amphoteric ionic monomer, *i.e.*, 3-(3-methylacrylamide propyl dimethylamino)-propyl-1-sulfonate (MEPS) in conventional acrylamide (AM) and acrylic acid (AA) enhanced the rheological properties of polymer flooding agents, thereby improving their temperature resistance and salt tolerance. A series of experiments were performed to determine the optimal reaction conditions for the polymer; the structure and molecular weight characteristics of MANPS were confirmed by FT-IR spectroscopy, ^{1}H NMR spectroscopy, intrinsic viscosity, high-performance liquid chromatography (HPLC) and SEM. The rheological test results showed that MANPS had higher apparent viscosity than the partially hydrolyzed polyacrylamide (HPAM). It exhibited good shear recovery at a certain shear rate. The reason was considered to be the long-chain entanglement of molecules and the "anti-polyelectrolyte action" of zwitterions. Thermogravimetric analysis provided good evidence of the thermal properties of the copolymer MANPS. Evaluating the oil displacement performance of the oil-displacing agent was an essential part. The results showed that the copolymer MANPS was comparable to HPAM having a 10.4% higher oil displacement rate under the same concentration and test conditions.

1 Introduction

In recent years, oil has been an irreplaceable necessity for human life, such as in the fields of fuels, plastics, asphalt, clothing and scientific research.[1,2] However, the production of oil has not fully met the current needs. Fortunately, some reliable studies have indicated that much of the crude oil in the formation can be effectively extracted by polymer flooding.[3–5] For polymer flooding, the viscosity and viscoelasticity of the displacement solution are two key factors. The reason is that the polymer flooding technology to enhance oil recovery is mainly conducted by increasing the sweep volume and displacement efficiency of the displacement solution.[6,7] Partially hydrolyzed polyacrylamide (HPAM)[8,9] as the commonly used polymer for enhanced oil recovery (EOR) often suffers a significant decrease in its own viscosity[10,11] due to the high temperature and high salinity of the formation.[12–15] Consequently, it is of great importance to develop novel HPAM substitutes with good viscosity and viscoelasticity even under high-temperature and high-salinity conditions.

On the other hand, according to the oil-displacement mechanism, it is inevitable that the oil-displacing polymer should have good rheological properties.[16–20] Many studies have reported that by introducing hydrophobic groups or anionic and cationic groups into the HPAM molecular chain, the temperature and salt resistance of the polymer can be effectively improved through intermolecular interactions (hydrogen bonds, van der Waals forces, Coulomb forces, *etc.*).[21–23] Furthermore, due to the hydrophilic macromolecule chain and a small amount of hydrophobic groups of the hydrophobically associating polymer, this kind of polymer solution has unique properties.[24,25] In order to further improve the rheological properties of the HPAM substitutes, an effective method is to introduce some anionic and cationic groups and hydrophobic groups to form a novel zwitterionic polymer.

Lately, articles on amphoteric ionic polymers have been widely reported. Banerjee *et al.*[26] successfully synthesized an L-lysine-based amphoteric ionic polymer (PLAM) by water-based synthesis and found that under different acid–base conditions, the polymer (PLAM) could interact with Cu(II) ions to form spherical aggregates or dissociate into free polymer chains. Zheng *et al.*[27] reviewed the application progress of an amphoteric ionic

[a] *Oil and Gas Field Applied Chemistry Key Laboratory of Sichuan Province, Southwest Petroleum University, Chengdu 610500, China*
[b] *State Key Laboratory of Oil and Gas Reservoir Geology and Exploitation, Southwest Petroleum university, Chengdu 610500, China*
[c] *Henan Energy and Chemical Group Co., Ltd, China*

† Electronic supplementary information (ESI) available. See DOI: 10.1039/d0nj01687j

polymer at the molecular level and pointed out that the amphoteric ionic polymer has great development potential in the future. Ibrahim *et al.*[28] synthesized amphoteric polymer nanoparticles *via* distillation–precipitation polymerization (DPP) using [2-(methyl propylene oxide) ethyl] dimethyl sulfur propyl (3-) ammonium hydroxide (SBMA) as the monomer and *N*,*N*′-methylene double (acrylamide) (MBAAm) as the crosslinking agent. Blackman *et al.*[29] summarized the structure of different amphoteric ion monomers and the preparation methods of their polymers. In addition, their response behavior and potential applications under different environmental stimuli (temperature, pH, salt, and dual-reaction systems) were summarized.

In this article, a zwitterionic polymer containing a hydrophobic long chain, named MANPS, was independently developed by free radical solution polymerization using octadec-9-enioc acid allylamide (NAE) as a hydrophobic monomer. The polymerization conditions and solution properties of MANPS were investigated. We analyzed the synthesized amphoteric ionic monomer 3-(3-methylacrylamide propyl dimethylamino)-propyl-1-sulfonate (MEPS) using FT-IR and ^{1}H NMR, and determined the FT-IR, ^{1}H NMR, SEM and intrinsic viscosity of MANPS. In addition, a series of rheological tests proved that MANPS had good temperature resistance, salt tolerance, shear recovery and thixotropy. It was proved by a simulated flooding experiment that this novel polymer MANPS can enhance oil recovery in harsh reservoir environments.

2 Experimental section

2.1 Materials

Acrylamide (AM), acrylic acid (AA), sodium hydroxide (NaOH), ammonium persulfate ($(NH_4)_2S_2O_8$), sodium hydrogen sulfite ($NaHSO_3$), sodium chloride (NaCl), magnesium chloride ($MgCl_2$), calcium chloride ($CaCl_2$), *N*-[3-(dimethylamino)propyl]methacrylamide, 1,3-propyl sulfonolactone and 4,4′-methylenebis(2,6-di-*tert*-butylphenol) were purchased from Chengdu Kelong Chemical Reagents Corporation (Chengdu, China). HPAM, with a relative molecular weight of about 1.3×10^7, was from Daqing Refining & Chemical Company (China). The functional sulfonate monomer MEPS was prepared in the laboratory. The hydrophobic monomer NAE was prepared according to the literature.[30]

2.2 Synthetic methods

2.2.1 Synthesis of MEPS. The reaction route of MEPS is clearly shown in Fig. 1(a): 16.83 g of *N*-[3-(dimethylamino)propyl]methacrylamide, 40 mL of 1,3-propyl sulfonolactone and 0.05 g of 4,4′-methylenebis(2,6-di-*tert*butylphenol) were added to a 250 mL three-necked round bottom flask with an appropriate amount of deionized water. After heating to 55 °C under oil bath conditions, a mixture of vinyl sulfite inner salt (11.01 g) (according to the literature method[31]) and 1,3-propyl sulfonolactone were slowly added to the flask through a constant pressure dropping funnel for 4 h. Finally, the white powdery vinyl sulfite inner salt MEPS was obtained by reduced pressure distillation.

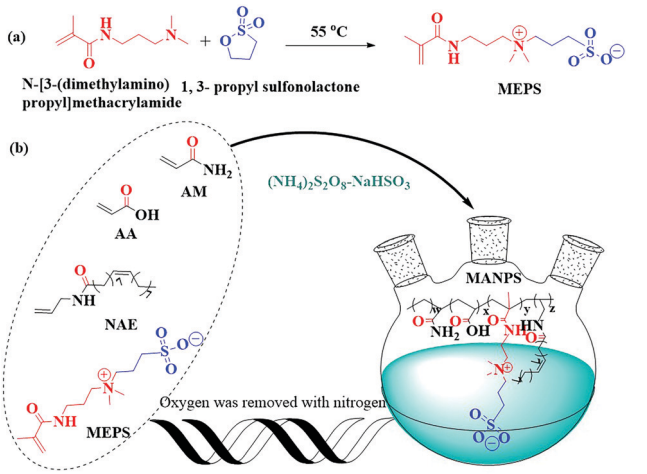

Fig. 1 The synthetic routes for (a) MEPS, (b) MANPS.

2.2.2 Synthesis of the copolymer MANPS. The final product, MANPS, was synthesized by free radical solution polymerization based on the work above, and the reaction route is given in Fig. 1(b). According to the optimization results of Tables S1 and S2 (ESI†), the detailed reaction steps are given. In brief, AM, AA, functional monomer MEPS and NAE were added to a triple flask containing 40 mL distilled water at a molar ratio of 330 : 140 : 1.5 : 1. After being adjusted to a pH of 7, the solution was then transferred to a super thermostatic water bath. Initiators $(NH_4)_2S_2O_8$ and $NaHSO_3$ accounted for 0.0642‰ of the total moles of monomer (the molar ratio was controlled at 1 : 1) were added into the reaction system under a nitrogen atmosphere at the indicated temperature. After reacting for 8 h at 50 °C, the copolymer gels were precipitated and washed with anhydrous ethanol to remove the unreacted monomers and initiators, and then dried at 60 °C in a vacuum for 10 h to obtain the corresponding copolymers, MANPS.

2.3 Characterization

FT-IR spectra of the samples were obtained *via* a WQF-520 Fourier transform infrared spectrometer in the optical range of 4000–500 cm^{-1}. ^{1}H NMR spectra were measured on a Bruker AM 400 MHz NMR spectrometer using D_2O as the solvent. The intrinsic viscosity of the MANPS copolymer was determined by the dilution method[32] with an NCY automatic Ubbelohde capillary viscometer (0.55 mm) (Shanghai Sikeda Scientific Instruments Inc., Shanghai, China) at 30 ± 0.1 °C. Copolymer composition was determined by HPLC (LC-20A, Hitachi, Tokyo, Japan). The test conditions were set as follows: ODS column, V(H_2O) : V(CH_3OH) = 1 : 9, 210 nm, 40 °C, 1.0 mL min^{-1}. Scanning electron microscopy (SEM) analyses of HPAM and MANPS were acquired with an FEI Quanta 450 (FEI, USA). TG-DTG was carried out on an STA449 F3 synchronous thermal analyzer under a nitrogen flow rate of 60 mL min^{-1} with the heating rate of 10 °C min^{-1}. It is worth noting that the temperature range was 40–800 °C.

2.4 Rheological properties

2.4.1 Viscoelasticity. Two kinds of 2000 mg L^{-1} solution of polymer HPAM and MANPS were prepared in simulated

Table 1 Ionic composition of the simulated stratum water

Inorganic ions	Na^+	Mg^{2+}	Ca^{2+}	Cl^-	CO_3^{2-}	HCO_3^-	SO_4^{2-}
Content (mg L^{-1})	2903	150	236	5185	164	285	100

brine (Table 1). In order to ensure consistent experimental conditions, the experimental temperature was set to 25 °C, and the storage modulus (G') and the energy dissipation modulus (G'') of the copolymer solution were tested by a HAAKE MARS III rheometer.

2.4.2 Thixotropy. The formation and destruction of the structure of MANPS were characterized by thixotropy. The area between the upper and lower curves reflects the thixotropy of MANPS. In the first stage, the shear rate increased from 0.01 s^{-1} to 10 s^{-1}. In the second stage, the shear rate was maintained at 0 s^{-1} for 40 seconds. In the third stage, the shear rate was reduced from 10 s^{-1} to 0.01 s^{-1}. In this experiment, the MANPS solution was measured by adjusting three parameters in the rotary mode on a HAAKE MARS III rheometer.

2.4.3 Shear reversibility and shear thinning. When a polymer solution is injected into the formation, its molecular structure is easily broken due to the high shear rate, resulting in a lower apparent viscosity and a decreased efficiency in the oil displacement. On this basis, both copolymer solutions, HPAM and MANPS, with mass concentration of 2000 mg L^{-1} were sheared under certain steps. The specific steps were as follows. (1) Continuous shearing at 25 °C for 3 min at 170 s^{-1}. (2) The shear rate changed to 510 s^{-1} for shearing for 3 min. (3) The shear rate decreased to 170 s^{-1} for 3 min of continuous shearing. (4) Both (1) and (2) were repeated and the apparent viscosity of the copolymer solution was observed. The polymer was formulated into a 0.1% solution and its apparent viscosity was measured by a HAAKE MARS III rheometer at different shear rates.[33–35]

2.4.4 Apparent viscosity. The polymers HPAM and MANPS were prepared in brine to a concentration of 2000 mg L^{-1}, then the apparent viscosity of the polymer solution under different conditions (such as temperature, salt solution concentration) were tested using a HAAKE MARS III rheometer.

2.5 Displacement experiment

The displacement efficiencies of the two polymers, HPAM and MANPS, were evaluated by core flooding experiments. The injection pressure was recorded to calculate the resistance factor (RF) and residual resistance factor (RRF), and the method to obtain the results was as follows:

$$RF = \frac{P_p/Q_p}{P_{ws}/Q_{ws}} \quad (1)$$

$$RRF = \frac{P_{wf}/Q_{wf}}{P_{ws}/Q_{ws}} \quad (2)$$

where P_p and P_{ws} (MPa) are the stable pressures of the copolymer solution and the saturated salt solution, respectively. Q_p and Q_{ws} (mL min^{-1}) are the injection rates of the copolymer solution and the saturated salt solution. P_{wf} (MPa) is the stable pressure of water flooding. Q_{wf} (mL min^{-1}) is the injection rate of water flooding. A salt solution of a copolymer of 2000 mg L^{-1} was prepared. The ionic composition of the simulated stratum water can be seen in Table 1.

First, the water flooding was carried out at a speed of 0.7 mL min^{-1} until the water content reached 99%. The copolymer solution was then injected for displacement at the rate of 0.7 mL min^{-1}. Finally, the water flooding was performed again until the water content was 99%. The EOR percentage was obtained as follows:

$$EOR = E - E_w \quad (3)$$

where EOR (%) is the enhanced oil recovery; E (%) is the oil recovery of the whole displacement process; E_w (%) is the oil recovery of water flooding.

3 Results and discussion

3.1 Characterization

Before the tests below, the influencing conditions, such as monomer ratio, initiator ratio, temperature and pH, *etc.*, of the synthetic polymer MANPS were optimized through experiments. The specific optimization schemes are shown in Tables S1 and S2 (ESI†), and Table 2 gives the optimal reaction conditions.

3.1.1 FT-IR spectra of MEPS and MANPS. Thin slices of the purified MEPS and MANPS were prepared through mixing with dried KBr to investigate the FT-IR spectra using a Fourier infrared spectrometer, as shown in Fig. 2. For MEPS, the stretching vibration absorption peak of N–H in –C(O)–NH– in MEPS was at 3477 cm^{-1}. A distinct stretching vibration peak assigned to C–H in MEPS was at 2977 cm^{-1} and peaks at

Table 2 The optimal reaction conditions of synthetic MANPS

AM : AA : MEPS : NAE[a]	Initiators (‰, molar)	pH	T/°C
330 : 140 : 1.5 : 1	0.0642	7	50

[a] The ratios are the molar ratios.

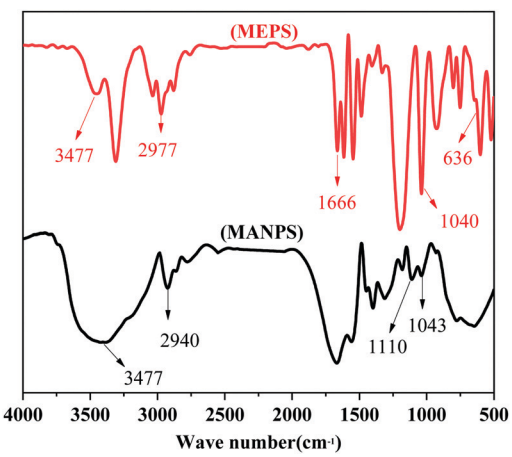

Fig. 2 FT-IR spectra of MEPS and MANPS.

1666 cm^{-1} and 1040 cm^{-1} belonged to C=C and C=O, respectively. The copolymer MANPS exhibited strong absorption peaks at 3417 cm^{-1}, 1665 cm^{-1} and 1110 cm^{-1}, which respectively reflected the peak spectra of –OH, C=O and S=O. Additionally, another peak appeared at 636 cm^{-1}, which was the bending vibration absorption peak of N–H in the amide. Based on IR spectroscopy, the sample structure was in line with the designed macromolecular structure, indicating that the functional monomer MEPS was successfully introduced into the backbone of MANPS, and the expected effect was achieved.

3.1.2 ^{1}H NMR spectra of MEPS and MANPS. In order to describe the structures and purity of the monomer MEPS and copolymer MANPS more accurately, we conducted nuclear magnetic tests on these two substances, and the test results are shown in Fig. 3. As illustrated in Fig. 3(a), the ^{1}H NMR spectrum of the monomer MEPS was given. The chemical shifts at δ = 5.52 ppm and 5.76 ppm were attributed to the unsaturated olefin hydrogen –C(CH$_3$)=CH_2 proton peak, and the chemical shift at δ = 3.00–3.04 ppm was attributed to the –CH$_2$–CH_2–SO$_3$– proton peak. The proton signals at 3.39–3.40 ppm showed the existence of –C(O)–NH–CH_2– groups. The chemical shift at δ = 3.15 ppm was attributed to the –N$^+$(CH_3)$_2$– proton peak, and the chemical shift at δ = 3.42–3.54 ppm was attributed to –CH$_2$–N$^+$(CH$_3$)$_2$–CH_2–. The proton signals at 2.06–2.12 ppm were due to –C(O)–NH–CH$_2$–CH_2– groups. The chemical shift at δ = 1.97 ppm was attributed to the –CH$_2$=C(CH_3)– proton peaks. The proton signals at 2.23–2.29 ppm were due to –CH_2–CH$_2$–SO$_3$– groups.

The ^{1}H NMR spectrum of MANPS is shown in Fig. 3(b). It can be seen that the –CH=CH– protons in the NAE monomer appeared at δ = 5.16 ppm. The proton signal at 3.57 ppm was due to –CH_2–N$^+$(CH$_3$)$_2$–CH_2– groups. The signal at δ = 3.29 ppm was due to the proton in –CH_3 connected to N$^+$ and in –CH_2 connected to –NH. The chemical shift at δ = 3.07 ppm was attributed to the –CH$_2$–CH_2–SO$_3$– proton peak. The proton signal at 2.50 ppm was due to –CH_2–CH$_2$–SO$_3$– groups. Additionally, the existence of the proton peak at δ = 2.36 ppm was due to –CO–NH–CH_2–. The proton signal at 1.98–2.03 ppm showed the existence of [NH$_2$–CO–CH–] groups and it was obvious that the protons of the –CH_2– group of the main copolymer chain appeared at 1.44 ppm. The proton peak at δ = 0.84 ppm was due to –CH_3 connected to –(CH$_2$)$_7$– groups.

3.1.3 Intrinsic viscosity measurement of MANPS. Intrinsic viscosity is an effective method for characterizing molecular weight.[36,37] According to the data (Table S3, ESI†), the relationship curves of η_{sp}/C *vs.* C and $(\ln\eta_r)/C$ *vs.* C are described in Fig. 4. Combining Fig. 4 and the formulae $\eta_r = t/t_0$, $\eta_{sp} = \eta_r - 1$ and $[\eta] = H/C_0$, it was determined that the intrinsic viscosity number of MANPS was 772 mg L^{-1}.

3.1.4 Composition measurement of MANPS. High-performance liquid chromatography (HPLC) is often used to detect the composition of polymers.[39] Here, the standard curve for each monomer was determined as $A_{AM} = 4.2582 \times 10^7 \times \rho + 31\,4374.5$; $A_{AA} = 1.2982 \times 10^7 \times \rho + 38\,643.6$; $A_{MEPS} = 4218.56 \times \rho + 1105.9$. Further, the conversion ratio of each component and its proportion in the copolymer were calculated from formula (4), and the results are shown in Table 3.

$$\alpha = \frac{W - \frac{A\rho_0}{A_0} \times V}{W} \times 100\% \quad (4)$$

α is the monomer conversion rate (%); W is the monomer raw charge quality (g); A is the monomer peak area in the chromatogram of the ethanol used for purifying the polymer; ρ_0/A_0 is

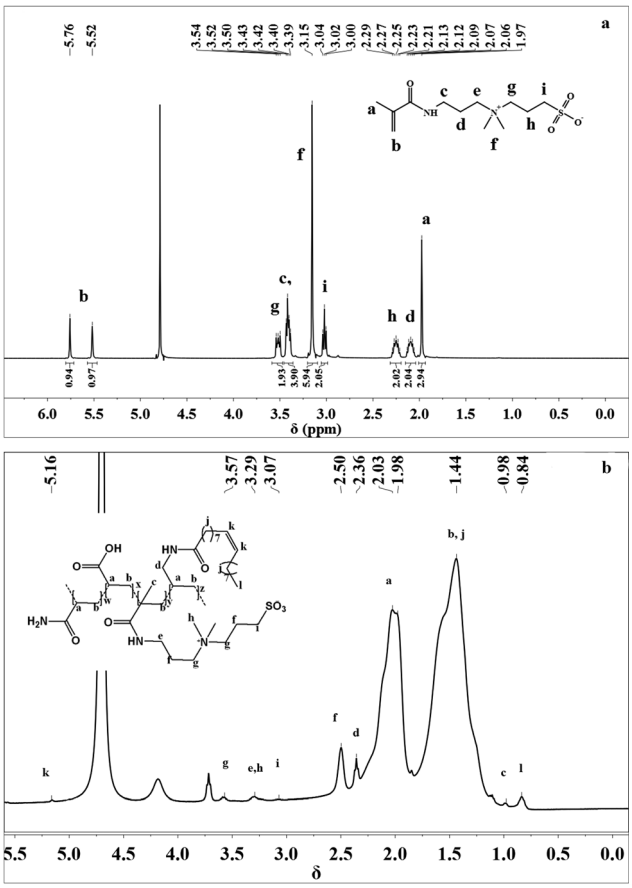

Fig. 3 ^{1}H NMR spectra: MEPS (a) and MANPS (b).

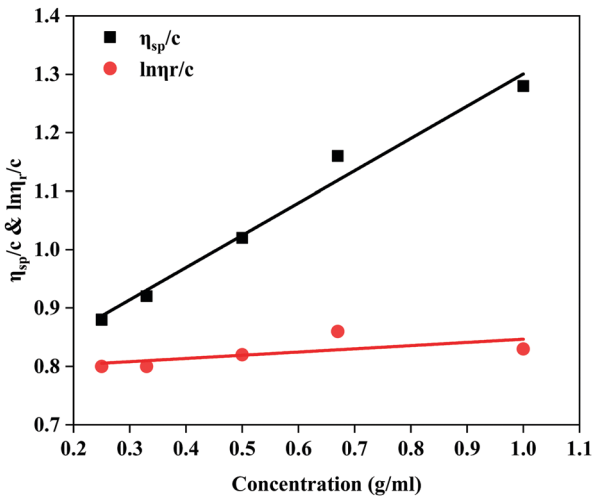

Fig. 4 The relationship curves of η_{sp}/C *vs.* C and $(\ln\eta_r)/C$ *vs.* C.

Table 3 The composition of copolymer MANPS[a]

	Molar ratio of reactants (%)				Molar composition (%)			
Entry	AM	AA	MEPS	NAE	AM	AA	MEPS	NAE
MANPS	69.93	29.56	0.28	0.23	69.99	29.58	0.25	0.18

[a] All data are the average of three measurements with an error of ±0.1.

the reciprocal of the slope of the monomer standard curve; V is the total volume (L) of ethanol used to purify the polymer.

3.1.5 Thermogravimetric testing of MANPS. TG-DTG was used to investigate the thermal stability of MANPS, and Fig. 5 shows the experimental results. As we all know, the decomposition temperature of the polymer depends greatly on its molecular mass and molecular structure. The addition of long-chain hydrophobic groups and sulfonic acid groups allows the polymer to have more excellent thermal stability. The results can be described in five stages of weight loss.

The first weight-loss stage with 4.69% was at 43–173 °C, which can be attributed to the loss of water, ethanol and other small molecules. The second stage was at 173–277 °C, with a 7.42% weight loss rate, which was estimated to be the decomposition of the side group, macromolecular chain and branching of MANPS. The third stage of weight loss at 277–383 °C was for the decomposition of the polymer backbone. The fourth stage occurred at 383–618 °C, which was probably due to the carbonization of the polymer particles. The last stage of weight loss caused by the further carbonization of polymer particles was above 618 °C.

3.1.6 SEM of HPAM and MANPS. The polymers were dissolved in 1% NaCl solution then freeze-dried to obtain micromorphological images of HPAM and MANPS by SEM; the results are shown in Fig. 6.

Intuitively, the microscopic appearance of both polymers showed a network structure with attached backbones. Most notably, the linkage backbone of HPAM was significantly weaker than that of MANPS with a distinct cavity network structure. This phenomenon can be attributed to the hydrophobic association, thus strengthening the tangle of molecular

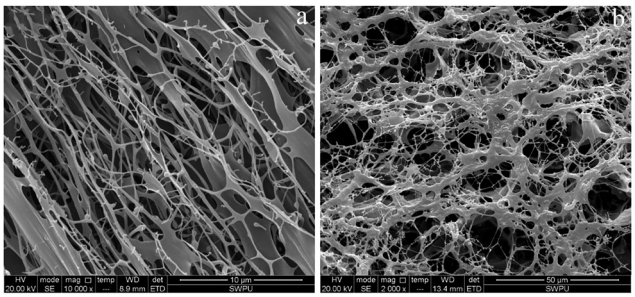

Fig. 6 SEM analysis of the polymers in 1% NaCl solution: (a) HPAM; (b) MANPS.

chains and creating a more robust backbone connection. In addition, the molecular chains in Fig. 6(a) were sparsely distributed without forming many crosslinking points or entangling with each other. In contrast, the branched chains in Fig. 6(b) were entangled with each other, thus forming a dense crosslinking network. The different micromorphologies of the two polymers indirectly confirmed the feasibility of the experiment and indicate the potential for the excellent properties of MANPS.

3.2 Rheological properties analysis of HPAM and MANPS

3.2.1 Viscoelasticity. The viscoelasticity of oil displacing agents is of great importance for oil displacement performance,[40] and different fluids have different flow viscoelastic characteristics. The viscoelastic properties of the copolymer solution can be characterized by the storage modulus (G') and the loss modulus (G''). G' corresponds to the elasticity of the system and G'' corresponds to the viscosity of the system. The relationships between MANPS and HPAM modulus and strain were shown in Fig. 7.

As shown in Fig. 7, at the scanning frequency of 0.1–10 Hz, with increased scanning frequency, the long molecular chains were more severely entangled, the storage modulus (G') and the energy dissipation modulus (G'') of HPAM and MANPS both showed a gradual increase. At the scanning frequency of 0.1–0.5 Hz, the growth of G' of the copolymer MANPS was larger than that of G'', and $G' < G''$, indicating that the copolymer

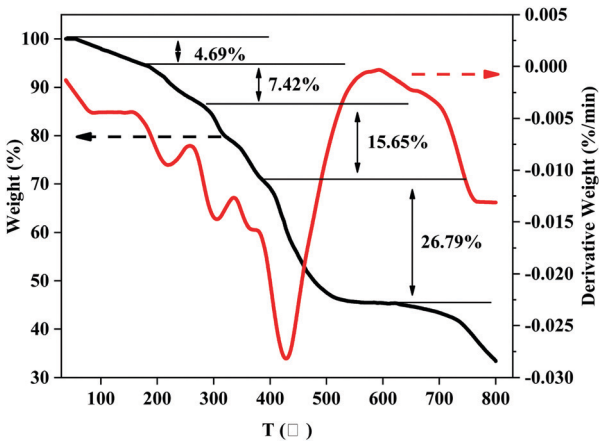

Fig. 5 TG-DTG of MANPS.

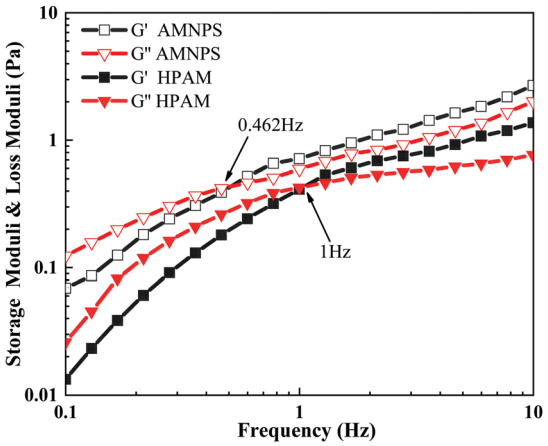

Fig. 7 Viscoelasticity of HPAM and MANPS.

solution was mainly viscous at low frequencies. However, when the scanning frequency exceeded 0.462 Hz ($G' > G''$), the solution of copolymer MANPS showed mainly elasticity at high frequencies. However, for HPAM, the demarcation point frequency at viscosity and elasticity occurred at 1 Hz. In addition, in the scanning frequency range of 0.1–10 Hz, the G' and G'' of the MANPS copolymer were higher as compared to HPAM, and the solution of MANPS demonstrated obvious elasticity at lower frequencies, which was more conducive to improving the oil displacement performance of the polymer solution. The reason the viscoelasticity of MANPS was better than that of HPAM was mainly that its hydrophobic groups aggregated in aqueous solution owing to hydrophobic interactions, thus inducing the separation of macromolecular chains. Intermolecular association generated a stable physical cross-linking network, which allowed MANPS to have excellent viscoelasticity.

3.2.2 Thixotropy. Good thixotropy provides the oil displacement agent with good pumping performance and oil displacement performance. Therefore, in order to test the thixotropy of the polymers, thixotropy experiments had been done.[47,48] As shown in Fig. 8, the areas between the upper and lower curves reflect the thixotropy of the polymers. MANPS had a more pronounced thixotropic ring (Fig. 8a) as compared to HPAM (Fig. 8b). This was because the cross-linking of the MANPS system during the shearing process was reversible and recoverable, endowing MANPS with better thixotropy. On the other hand, with the increase in the shear stress, the intermolecular structure of the thixotropic fluid was destroyed. When the shear stopped, the structure between the molecules gradually recovered.

The larger area of the MANPS thixotropic ring indicated that the stability of the molecular structure of MANPS was better than that of HPAM. Moreover, from both figures we can see that the viscosity of both polymers decreased as the shear rate increased. However, when the shear rate gradually decreased, the viscosity of the two increased but the final viscosity value of MANPS was closer to the initial value. This shows that the cross-linked network formed by MANPS has a stable structure and strong spatial recovery, indirectly implying that the MANPS system would have excellent shear reversibility. Predictably, the use of the MANPS oil-displacing agent can greatly reduce the fluid flow resistance, which will make it more conducive to improving the displacement efficiency of low permeability reservoirs.

3.2.3 Shear reversibility and shear thinning

Shear reversibility. When the polymer solution is injected into the formation, due to the high shear rate, the easily broken molecular structure will lead to a lower apparent viscosity,[41] resulting in a decrease in the oil displacement efficiency. Therefore, for the polymer to have excellent performance, on the one hand, it should have good shear sensitivity; on the other hand, its structure should not be destroyed. Fortunately, from the thixotropy experiment, we found that MANPS had good shear reversibility, and may be different from HPAM to some extent. The curves of the shear recovery of the polymers are shown in Fig. 9a. When the shear rate suddenly changed from 170 s^{-1} to 510 s^{-1}, the viscosity of the polymer solution decreased significantly, which was attributed to the destruction of the associated spatial network structure under high shear. Nevertheless, when the shear rate recovered from 510 s^{-1} to 170 s^{-1}, thanks to the re-formation of the space network, the viscosity of the polymer solution recovered immediately (Fig. 9a). For the MANPS polymer solution, the viscosity recovery rate reached 98.9% as compared to 96.9% for HPAM, indicating that MANPS performed better in shear recovery.

Shear thinning. As can be seen from Fig. 9b, when the shear rate increased, the apparent viscosity of both polymer solutions decreased rapidly. When the shear rate increased to 100 s^{-1}, the apparent viscosity of the polymer solution decreased gently; when the shear rate reached 505 s^{-1}, the viscosity of the polymer solution was 33.87 mPa s, which was higher as compared to 14.08 mPa s of HPAM. The decline in the viscosity of MANPS was 93.30%, while the decline in that of HPAM reached 94.35%, showing that the two polymers both had good shear thinning performance.

In summary, the excellent shear sensitivity and shear recovery properties of MANPS help it maintain a high viscosity and smoothly reach the formation without the effect of the high-speed rotation of the injection equipment.

3.2.4 Evaluation of the salt-resistance and temperature-resistance. In view of the high-temperature and high-salinity conditions of the oil-bearing reservoir, it is necessary to simulate the formation environment for the polymer viscosity test.[38] It is important to note that the shear rate was set at 7.34 s^{-1}.

Salt-resistance. In general, from Fig. 10a–c, the apparent viscosity of the MANPS solution began to show a decline with the increase in salinity, and then the downward trend suddenly subsided and some hills were seen due to the effect of the anti-polyelectrolyte. After the anti-polyelectrolyte effect, the viscosity dropped sharply and finally became stable. When NaCl, $CaCl_2$ or $MgCl_2$ (Fig. 10a–c) was added to the polymer solution, the viscosity retention of the MANPS solution was 50.67 mPa s,

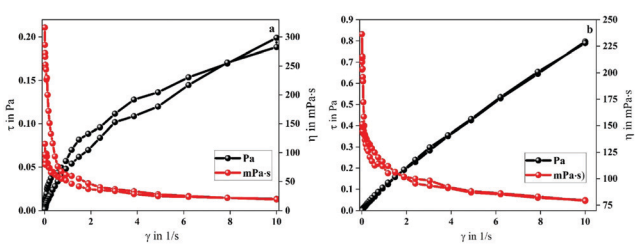

Fig. 8 Comparison of the thixotropy of (a) MANPS and (b) HPAM.

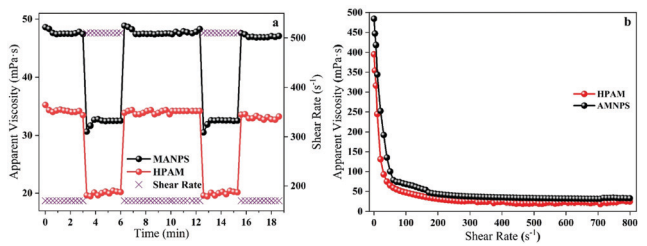

Fig. 9 The shear reversibility (a) and shear sensitivity (b) of the polymers.

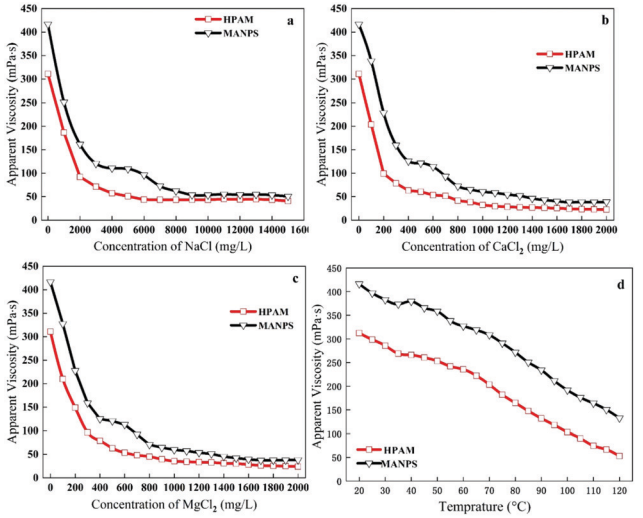

Fig. 10 Anti-Na^+ (a), Ca^{2+} (b), Mg^{2+} (c) performance of the polymer solution; polymer temperature resistance performance evaluation (d).

38.9 mPa s and 38.04 mPa s, respectively (which was higher as compared to 40.59 mPa s, 22.67 mPa s, 23.98 mPa s for HPAM). This suggests that the salt resistance of MANPS was better than that of HPAM. Additionally, it is important to note here that the zwitterionic polymer MANPS had equal numbers of anions and cations,[42,43] which can cause the inner chain anions and cations in the deionized water to attract each other and bend the molecular chain, leading to small hydrodynamic volume and low viscosity. However, in salt solution, the unequal numbers of zwitterions weakened the attraction of the inner chain of the molecule and the hydrodynamics interaction did not decrease but rise, showing the anti-polyelectrolyte effect.[44] This result can be explained by the fact that under the action of the inorganic salt, the polarity of the solution was increased to enhance the hydrophobic association of the molecular side chains, and the structural strength of the dynamic physical crosslinking network was increased.

Temperature-resistance. The experiment describes the change in the apparent viscosity of the 2000 mg L^{-1} MANPS polymer solution at different temperatures as compared with the HPAM solution.

The trend of the apparent viscosity with the change in temperature is shown in Fig. 10d. At 7.34 s^{-1}, the apparent viscosity of HPAM and MANPS decreased with the increasing temperature but the apparent viscosity of MANPS was always higher than that of HPAM at the same temperature (Fig. 10a). This was because the physically cross-linked network structure of MANPS was more robust, so the degree of destruction was lower than that of HPAM. As the temperature reached 90 °C, the apparent viscosity of MANPS was 50.3 mPa s, which was higher than 25.0 mPa s of HPAM. When the temperature was 120 °C, the apparent viscosity of the MANPS was 45.8 mPa s, which was also higher than the 23.6 mPa s of HPAM. This phenomenon showed that MANPS had a significant improvement in temperature resistance as compared to HPAM.

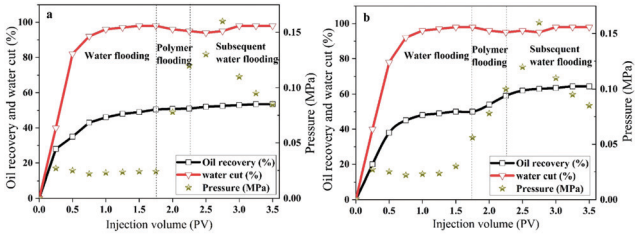

Fig. 11 The flooding capability of polymers: HPAM (a); MANPS (b).

3.3 Enhanced oil recovery of HPAM and MANPS

To compare the displacement effects of the two polymers HPAM and MANPS, a core displacement experiment was performed, and the results are shown in Fig. 11. Apparently, at the beginning of the injection, the water content, injection pressure and oil recovery rate all showed a sharp rise and then gradually stabilized with the injection of simulated formation water in the water flooding stage. The water drive of each core was harvested, and the oil recovery rates were 50.5% (a) and 50.0% (b), respectively. When the oil recovery rate could no longer increase in water flooding, the copolymer salt solution was injected into the cores, resulting in a larger injection pressure. With the decrease in the water content, the oil recovery of the HPAM and MANPS salt solution reached 51% (Fig. 11a) and 59% (Fig. 11b), respectively, in the polymer injection stage. Correspondingly, HPAM and MANPS increased the recovery to 53.5% and 64.4% in the final stage. Consequently, HPAM and MANPS can respectively increase oil recovery by 3.0% and 13.4%, which indicate that copolymer MANPS had the greater potential in practical oil flooding applications. Copolymer MANPS produced a hydrophobic association effect in aqueous solution,[45,46] which made it retain high viscosity under high temperature and high salinity conditions, effectively reducing the oil–water mobility ratio and thus carrying more residual oil to improve the oil displacement performance.

4 Conclusions

In this work, a zwitterionic polymer, MANPS, containing a hydrophobic long chain was prepared from AM, AA, NAE and MEPS. Its good rheological properties, thixotropic properties and shear recovery properties endowed it with huge potential for EOR. Its good temperature resistance and salt tolerance made it resistant to the high temperature and high salinity of the formation. The effects of the monomer addition ratio, reaction temperature, initiator addition amount and pH on the polymer were investigated systematically. FT-IR, ^{1}H NMR, intrinsic viscosity, HPLC and SEM were applied to characterize the structure and molecular weight of MANPS. The viscoelasticity test results showed that the polymer had excellent viscoelastic properties. At the shear rates of 0.01 s^{-1} to 10 s^{-1}, MANPS had better thixotropic properties than HPAM. At a shear rate of 505 s^{-1}, the viscosity of the MAPNS solution was 33.87 mPa s, and the decline in the viscosity was 93.30%; at a shear rate of 170 s^{-1}, the viscosity of the zwitterionic polymer

was 47.1 mPa s at 120 °C, indicating its good shear sensitivity. Thermogravimetric analysis showed that the copolymer had good thermostability. The rheological results exhibited that when a certain amount of NaCl, $CaCl_2$ and $MgCl_2$ were added to the polymer solution, the viscosity retentions of the MANPS solution were 50.67 mPa s, 38.9 mPa s and 38.04 mPa s, respectively. The simulated oil displacement experiment showed that MANPS had a 10.4% higher oil displacement rate under the same concentration and test conditions as compared to HPAM, which indicates its potential for oil displacement.

Conflicts of interest

There are no conflicts to declare.

Acknowledgements

This work is supported by Southwest Petroleum University Graduate Teaching and Research Teaching Reform Project [18YJYB16], Science and Technology Innovation Seedling Project of Sichuan Province [2019092] (China). We also would like to express our gratitude to the editors and reviewers for the recommendations to improve the quality of this work.

Notes and references

1 W. T. Frankenberger and J. B. Johanson, *J. Environ. Qual.*, 1982, **11**, 602–607.
2 V. E. Galtsev, I. M. Ametov and O. Y. Grinberg, *Fuel*, 1995, **74**, 670–673.
3 J. Yao, X. Deng, Y. Zhao, T. Han, M. Chu and J. Pang, *Pet. Explor. Dev.*, 2013, **40**, 161–169.
4 M. Chahardowli, R. Farajzadeh and H. Bruining, *J. Ind. Eng. Chem.*, 2016, **38**, 50–60.
5 J. Sun, W. Du, X. Pu, Z. Zhou and B. Zhu, *Chem. Pap.*, 2015, **69**, 1598–1607.
6 V. C. Santanna, F. Curbelo, T. C. Dantas, A. D. Neto, H. S. Albuquerque and A. Garnica, *J. Pet. Sci. Eng.*, 2009, **66**, 117–120.
7 H. Liu, C. Xiong, Z. Tao, Y. Fan, X. Tang and H. Yang, *RSC Adv.*, 2015, **5**, 33083–33088.
8 S. Abdel-Azeim and M. Y. Kanj, *Energy Fuels*, 2018, **32**, 3335–3343.
9 A. Samanta, K. Ojha, A. Sarkar and A. Mandal, *Int. J. Oil Gas Coal Technol.*, 2013, **6**, 245.
10 X. Li, Z. Xu, H. Yin and Y. Feng, *Energy Fuels*, 2017, **31**, 2479–2487.
11 T. Li, T. Ci, L. Chen and L. Yu, *Polym. Chem.*, 2013, **5**, 979–991.
12 K. Spildo and E. I. Sæ, *Energy Fuels*, 2015, **29**, 5609–5617.
13 A. Ait-Kadi, P. J. Carreau and G. Chauveteau, *J. Rheol.*, 1987, **31**, 537–561.
14 K. C. Tam and C. Tiu, *Colloid Polym. Sci.*, 1994, **272**, 516–522.
15 A. Samanta, A. Bera and K. Ojha, *J. Chem. Eng. Data*, 2010, **55**, 4315–4322.
16 Z. Zhang, J. Li and J. Zhou, *Transp. Porous Media*, 2011, **86**, 199–214.
17 Y. Ruan, R. R. Davison and C. J. Glover, *Fuel*, 2003, **82**, 1763–1773.
18 K. Lewandowska, *J. Appl. Polym. Sci.*, 2007, **103**, 2235–2241.
19 Z. Zhang, J. Li and J. Zhou, *Transp. Porous Media*, 2011, **86**, 199–214.
20 M. S. Azad, Y. Dalsania and J. J. Trivedi, *Can. J. Chem. Eng.*, 2018, **96**, 2498–2508.
21 F. Candau, S. Biggs, A. Hill and J. Selb, *Prog. Org. Coat.*, 1994, **24**, 11–19.
22 N. Lai, W. Dong and Z. Ye, *J. Appl. Polym. Sci.*, 2013, **129**, 1888–1896.
23 G. Li, G. Zhang and L. Wang, *Energy Fuels*, 2013, **27**, 6632–6636.
24 C. Wang, T. Yang, T. Wang and L. W. Qiu, *Int. J. Biol. Macromol.*, 2018, **111**, 169–177.
25 J. Ma, P. Cui, L. Zhao and R. H. Wang, *Eur. Polym. J.*, 2002, **38**, 1627–1633.
26 S. Banerjee, T. Maji, T. K. Paira and T. K. Mandal, *Macromol. Rapid Commun.*, 2013, **34**, 1480–1486.
27 L. Zheng, S. S. Harihara, Z. Wei, C. Li and Z. Yuan, *React. Funct. Polym.*, 2017, **118**, 51–61.
28 G. P. S. Ibrahim, A. M. Isloor, Inamuddin, A. M. Asiri, N. Ismail, A. F. Ismail and G. Ashraf, *Sci. Rep.*, 2017, **7**, 15889.
29 L. D. Blackman, P. A. Gunatillake, P. Cass and K. Locock, *Chem. Soc. Rev.*, 2019, **48**, 757–770.
30 Z. Ye, M. Feng and S. Gou, *J. Appl. Polym. Sci.*, 2013, **130**, 2901–2911.
31 S. Gou, Y. He, L. Zhou, P. Zhao, Q. Zhang, S. Li and Q. Guo, *New J. Chem.*, 2015, **39**, 9265–9274.
32 P. Rani, G. Sen, S. Mishra and U. Jha, *Carbohydr. Polym.*, 2012, **89**, 275–281.
33 R. Zhao and C. W. Macosko, *J. Rheol.*, 2002, **46**, 145.
34 R. Zhao and C. W. Macosko, *AIChE J.*, 2007, **53**, 978–985.
35 L. Wang, J. Liu, S. Yuan, Y. Wang and Y. Xia, *Energy Environ. Sci.*, 2016, **9**, 224–231.
36 S. Fujishige, *Polym. J.*, 1987, **19**, 297–300.
37 T. H. Mourey, S. R. Turner and M. Rubinstein, *Macromolecules*, 1992, **25**, 2401–2406.
38 Q. Wu, S. Gou, Y. Fei, X. Yang, M. Liu and J. Huang, *Polymers*, 2019, **11**, 1781.
39 K. Hosoya, K. Yoshizako, Y. Shirasu, K. Kimata, T. Araki, N. Tanaka and J. Haginaka, *J. Chromatogr. A*, 1996, **728**, 139–147.
40 A. Viken, T. Skauge and K. Spildo, *J. Appl. Polym. Sci.*, 2016, **133**, 1097–4628.
41 F. Candau, S. Biggs, A. Hill and J. Selb, *Prog. Org. Coat.*, 1994, **24**, 11–19.
42 M. S. Kamal, A. S. Sultan, U. A. Almubaiyedh and I. A. Hussein, *Polym. Rev.*, 2015, **21**, 1–40.
43 P. Liu, Q. Chen, S. Wu, J. Shen and S. Lin, *J. Membr. Sci.*, 2010, **350**, 387–394.

44 G. S. George, E. B. Kamenska, E. D. Vassileva, I. P. Kamenova and V. T. Georgieva, *Biomacromolecules*, 2006, **7**, 1329–1334.
45 S. Kanagalingam, C. F. Ngan and J. Duhamel, *Macromolecules*, 2002, **35**, 8560–8570.
46 L. Zheng, S. S. Harihara, Z. Wei, C. Li and Z. Yuan, *React. Funct. Polym.*, 2017, **118**, 51–61.
47 J. Mao, H. Tan, B. Yang, W. Zhang, X. Yang, Y. Zhang and H. Zhang, *Polymers*, 2018, **10**, 2073–4360.
48 M. T. Ghannam, *J. Appl. Polym. Sci.*, 2009, **112**, 867–875.